

Article

A Multi-objective Scheduling Optimization Model for Hybrid Energy System Connected with Wind-Photovoltaic-Conventional Gas Turbines, CHP Considering Heating Storage Mechanism

Yao Wang ^{1,2,*}, Yan Lu ³, Liwei Ju ¹, Ting Wang ⁴, Qingkun Tan ¹ , Jiawei Wang ² and Zhongfu Tan ¹

¹ School of Economics and Management, North China Electric Power University, Beijing 102206, China; hdlwj@ncepu.edu.cn (L.J.); tanqingkun@ncepu.edu.cn (Q.T.); tzhf@ncepu.edu.cn (Z.T.)

² Economic and Electrical Research Institute of Shanxi Electrical Power Company of SGCC, Taiyuan 030002, China; wangjiawei@sx.sgcc.com.cn

³ State Grid Jibei Electric Economic Research Institute, Beijing 100095, China; hdluyan@163.com

⁴ Department of Power Engineering, Shanxi University, Taiyuan 030000, China; 201723503009@email.sxu.edu.cn

* Correspondence: wangyao@ncepu.edu.cn; Tel.: +86-153-3366-0900

Received: 25 December 2018; Accepted: 22 January 2019; Published: 29 January 2019



Abstract: In order to meet the user's electricity demand and make full use of distributed energy, a hybrid energy system (HES) was proposed and designed, including wind turbines (WTs), photovoltaic (PV) power generation, conventional gas turbines (CGTs), incentive-based demand response (IBDR), combined heat and power (CHP) and regenerative electric (RE) boilers. Then, the collaborative operation problem of HES is discussed. First, the paper describes the HES' basic structure and presents the output model of power sources and heating sources. Next, the maximum operating income and minimum load fluctuation are taken as the objective function, and a multi-objective model of HES scheduling is proposed. Then an algorithm for solving the model is proposed that comprises two steps: processing the objective functions and constraints into linear equations and determining the optimal weight of the objective functions. The selected simulation system is a microgrid located on an eastern island of China to comparatively analyze the influence of RE-heating storage (RE-HS) and price-based demand response (PBDR) on HES operation in relation to four cases. By analyzing the results, the following three conclusions are drawn: (1) HES can comprehensively utilize a variety of distributed energy sources to meet load demand. In particular, RE technology can convert the abandoned energy of WT and PV into heat during the valley load time, to meet the load demand combined with CHP; (2) The proposed multi-objective scheduling model of HES operation not only considers the maximum operating income but also considers the minimum load fluctuation, thus achieving the optimal balancing operation; (3) RE-HS and PBDR have a synergistic optimization effect, and when RE-HS and PBDR are both applied, an HES can achieve optimal operation results. Overall, the proposed decision method is highly effective and applicable, and decision makers could utilize this method to design an optimal HES operation strategy according to their own actual conditions.

Keywords: hybrid energy system; multi-objective model; heating storage; optimization scheduling

1. Introduction

Nowadays, energy and environmental pollution problems are getting more and more serious and people are paying attention to them. The role of distributed energy resources (DERs) in the

structure of power generation systems is increasing, especially wind and solar photovoltaic power generation. In particular, with the development of regenerative electric (RE) boiler technology, clean energy is no longer only used for power generation. It has also been gradually extended to heating sectors to form a thermal–electrical coupled operation mode. Meanwhile, combined heat and power (CHP) units are rapidly being more widely adopted due to the advantages of energy saving and environment friendliness [1]. However, due to the disadvantages of distributed energy sources, such as small capacity, intermittent availability, and dispersivity, they cannot be used in the electricity market alone, while the characteristics of CHP power generation closely combine with the supply of heating reduce the flexibility [2]. Therefore, the effective management of wind turbines (WTs), photovoltaic (PV) systems, and other distributed energy sources as well as CHP systems is urgently required to meet the current energy system needs and meeting this requirement has important theoretical and practical significance.

In recent years, the development and continuous maturity of virtual power plant (VPP) technology has provided a new means for the aggregation of distributed energy sources [3]. VPP technology does not change the use of a grid to connect distributed power sources; various types of distributed energy resources (DERs) are combined through advanced control, method of measurement, communication, and other technologies to achieve the coordinated optimization operation of multiple DERs and resources are rationally allocated through a higher level of software architecture [4]. For the analysis, a hybrid energy system (HES) is proposed, which controls the virtual power plant through the energy management system to realize the coordinated operation of CHP and DER.

The proposal of HES has received extensive attention at home and abroad. The German and Spanish governments jointly completed a virtual fuel cell power plant project. The project consisted of 31 CHP systems [5]. In 2007, the Netherlands established the HES program with 10 CHP units [6]. Cassell University in Germany has created the largest HES pilot project to combine wind turbines, solar systems, biogas power stations and hydropower stations [7]. In 2009, Danish Electric Vehicles considered the uncertainty of large-scale wind farms in the project of accessing smart grids, and the intelligent charging and discharging of electric vehicles was managed by HES technology [8]. In 2008, a distributed energy station was put into operation in Guangdong University City in China. The station uses a gas-steam combined cycle unit to generate electricity [9]. In 2014, China Power Corporation successfully connected a wind and solar project to the grid, and has already carried out business in Yunnan Province [10]. From 2010 to 2015, the EU conducted the WEB2ENERGY program, implemented and validated three intelligent technologies in intelligent power distribution, including smart metering, energy management and distribution automation [11].

Current research on HES economic operations at home and abroad mainly focuses on the electricity energy level, but the electrothermal coupling operation of HES with CHP is less considered. Zapata et al. [12] proposed an optimization model that can increase the revenue of the HES operation, and control the uncertainty of the wind power output by using a controllable load. Saeed et al. [13] analyzed coordination between solar photovoltaic power generation, wind power and hydropower. Moghaddam et al. [14] on the basis of fully considering the daily scheduling of HES components, proposed a hybrid integer linear programming (MILP)-based HES structure optimization method. Pandzic et al. [15] fully considered the influencing factors of the power market, using the MILP method to optimize the structure of HES. Wang et al. [16] proposed a method for scheduling and surging power in multiple HES cases, and also discussed the scheduling period. Carrion et al. [17] analyzed the scheduling and cost of small nuclear power plants and offshore wind farms. Erdinc [18] analyzed the economic impact of different demand response strategies in smart homes on storage units, small-scale self-generation and electric vehicles.

Previous research related to HES thermal–electrical coupled operation has mainly discussed the problem of coordinated operation of DERs and CHP, but has not discussed the aggregate utilization problem. Aboelsood et al. [19] considered the fluctuation of WT output and investigated the thermal–electrical scheduling problem of micro-grids (MGs) with WT and CHP. Zhang et al. [20]

developed an economic operation model for micro-grids with batteries and CHP in active power balance and reactive power balance. Aluisio et al. [21] discussed the application of CHP and energy storage technology in MGs, analyzed the effect of the time-of use (TOU) price on system operation, and comparatively analyzed the operation results of MGs with and without CHP. Taher et al. [22] proposed a combined optimization model of heat storage devices together with CHP. Mohammad et al. [23] developed an economic optimization model for a CHP-MG composed of a WT and fuel cells and solved the model by using an evolutionary algorithm. Furthermore, Wille-Hausmann et al. [24] combined CHP, and heating (HS) into an HES and discussed the thermal–electrical optimization scheduling problem. Giuntoli et al. [25] introduced an integrated dispatch model for CHP, WT, and HS. Manijeh et al. [26] developed an optimal operation model of an MG with CHP considering the revenue of supplying heating to establish the optimal operation strategy. [27] developed a nonlinear model based on the price elasticity of demand and benefit function of the customer. The behaviors of the derived models against elasticity change, incentive, penalty and potential of implementation are examined and degree of the reliance is determined. Reference [28] proposed a combination of these two programs with the merged program with incentive demand response, the time based demand response programs can be improved by using smart metering infrastructure and different resources. Reference [29] developed an incentive demand response with commercial energy management system based on diffusion model, smart meters and a new communication protocol.

The above studies have extensively discussed the optimization of the operation of HES, proposed a capacity allocation method for HES, and run optimization models and model solving algorithms. However, there are still some shortcomings. First, although there have been studies combining WT, PV, battery storage and CHP into HES, they have not considered the active response behavior of end customers, especially based on incentive demand response (IBDR), which can be involved in HES optimization operation and should be carefully considered. Secondly, previous studies related to the economic aspect of HES operation have mainly focused on the optimal strategy for integrating distributed power sources into a HES to meet terminal-customers' power demands, but they have failed to discuss the HS capability of RE technology, which could transfer electricity energy into heating energy for the optimal scheduling of the energy market. Thirdly, previous research has ignored the thermal-electrical synergy supply of CHP and RE. However, RE can be used to help manage electric power systems and heating systems, In particular, the heating storage capability could flatten the heating load demand curve; thus, it is urgent to study how the use of RE could influence HES operation. Based on the above analysis, we propose an optimized scheduling model for HES. The main results of this paper are as follows:

- We design a HES including WT, PV, conventional gas turbine (CGT), IBDR, RE and CHP. RE can convert electric energy into heating energy for thermal–electrical synergy supply. A multi-objective thermal–electrical scheduling model and an output model of power and heat sources are proposed.
- Based on the HES maximum operating income and minimum load fluctuation as the objective function, a multi-objective optimization model for HES thermoelectric scheduling is constructed according to the heating storage mechanism under the objective functions. Then, a model solution algorithm is proposed that comprises two steps: linearization of the objective functions and constraints and determination of the optimal weight coefficients of the objective functions.
- Four HES operation cases are set and the selected simulation system is a microgrid on an eastern island of China, validating the effects of the proposed models and algorithms. First, the four cases are set by considering the system without and with RE-HS and PBDR to analyze their combined optimization effect. Then, calculate the results of HES scheduling under various conditions, and compare and analyze the calculation results.

The rest of this article is as follows: The first part introduces the basic structure of multi-energy system (HES), the output model of power supply and heat source. The second section introduces the

multi-objective optimization model of HES scheduling based on the objective function of maximum operating income and minimum load fluctuation of HES. Next, the linearization method of objective functions and constraints as well as the weights calculation method of the objective functions are presented in Section 4. Then, the operation scenarios for HES are described for comparatively analysis in Section 5. At last, taking the microgrid built on an island in eastern China as an example, the microgrid is used as the simulation system to verify the proposed multi-objective model and solving algorithm, and verify its validity and applicability, in the Section 6. Section 7 emphasizes the contributions and conclusions of the paper.

2. Hybrid Energy System Structure Description

2.1. Basic Structure

In this study, WT, PV, CGT, CHP, RE, and IBDR are combined in a HES. RE, includes EB and HS, which could convert electric energy to heating energy. Then, to achieve the optimal operation, by using PBDR on the user side, not only can the load demand curve of power and heating be balanced, but also the grid space of WT and PV can be increased. Figure 1 shows a basic HES structure.

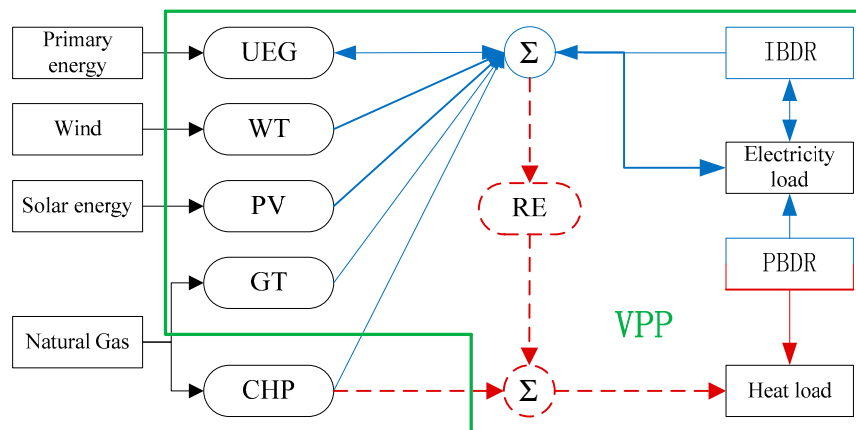


Figure 1. Basic structure of a hybrid energy system (HES).

The CHP operates in both a follow-up electrical load (FTL) and a follow-up thermal load (FTL) mode. WT, PV, gas turbine (GT), and CHP could meet the electricity load demand, but only RE and CHP can meet the demand of heating load. Therefore, in this work, CHP is set to operate in FTL mode to guarantee the reliability of supplying heating. Then, to maximize energy efficiency, WT, PV, and CHP are set to have high priority to meet the power load demand, while GT is set to provide auxiliary services for WT and PV. The demand for heating load is mainly provided by CHP, and if there is any remaining, it is provided by RE, which converts electric energy into heating energy.

2.2. Electricity Power Output Model

The main power sources of the HES include WT, PV, GT, IBDR, and CHP. However, in this work, CHP is designated as a heating source since CHP main users meet the demand for heating load.

2.2.1. WT Output

The main influencing factors of WT output power in natural customs. The randomness of the wind speed of natural winds leads to the random nature of the power everywhere. However, in [7], wind velocity was described as having a Rayleigh distribution:

$$f(v) = \frac{\varphi}{\vartheta} \left(\frac{v}{\vartheta}\right)^{\varphi-1} e^{-(v/\vartheta)^\varphi}, \quad (1)$$

where v is the real-time wind speed, φ is the form factor and ϑ is the scale factor. Simulate the distribution of natural winds by the average and variance of wind speed as shown in Equation (1). Then, calculate the output power of the WT by the following formula:

$$g_{W,t}^* = \begin{cases} 0, & 0 \leq v_t < v_{in}, v_t > v_{out} \\ \frac{v_t - v_{in}}{v_{rated} - v_{in}} g_R, & v_{in} \leq v_t \leq v_{rated} \\ g_R, & v_{rated} \leq v_t \leq v_{out} \end{cases}, \quad (2)$$

where g_W^* means the maximum output of the WT; g_R means the WT rated output; v is the real-time wind velocity, t means time; and in, rated, and out means the cut-in, rated, and cut-out, respectively.

2.2.2. PV Output

Solar radiation intensity will directly affect the output of photovoltaic power generation. Similarly, the random characteristics of PV radiation intensity lead to the random output of PV. In [7], it has been demonstrated that beta PDF can be used to distort the distribution of irradiance:

$$f(\theta) = \begin{cases} \frac{\Gamma(\alpha)\Gamma(\beta)}{\Gamma(\alpha)+\Gamma(\beta)} \theta^{\alpha-1} (1-\theta)^{\beta-1}, & 0 \leq \theta \leq 1, \alpha \geq 0, \beta \geq 0 \\ 0, & , otherwise \end{cases}, \quad (3)$$

where θ is the solar radiation intensity, α and β are the shape parameters of the beta distribution. The values of α and β can be obtained by the following formula:

$$\beta = (1 - \mu) \times \left(\frac{u \times (1 - \mu)}{\sigma^2} - 1 \right), \quad (4)$$

$$\alpha = \mu \left[\frac{\mu(1 - \mu)}{\sigma^2} - 1 \right], \quad (5)$$

where u and σ are the expected value and standard deviations of the PV radiation intensity, respectively. Further, according to the principle of photoelectric conversion, the PV output power can be obtained by the following formula:

$$g_{PV,t}^* = \eta_{PV} \times S_{PV} \times \theta_t, \quad (6)$$

where g^* represents the output power, η_{PV} represents the efficiency, S represents the total area, and θ is the radiation intensity.

2.2.3. Incentive-Based DR Output Model

In IBDR, users usually sign an agreement in advance. When the user is required to respond, the user needs to take corresponding response measures according to the content of the agreement signed by the user to adjust its power consumption and get compensation. Since the supply price of demand response determines the revenue of the Demand Response Provider (DRP), the DRP should not only consider the fluctuation of electricity market price but also the price of demand response when formulating IBDR plan [8]. Figure 2 shows the gradual price and demand curve for Demand Response (DR).

According to Figure 2, in step j , the minimum demand response is $D_i^{j,\min}$, and the largest demand response is $D_i^{j,\max}$. Therefore, DRP needs to participate in the scheduling of the energy market by meeting the following principles:

$$D_i^{j,\min} \leq \Delta L_{i,t}^j \leq D_{i,t}^j, j = 1, \quad (7)$$

$$0 \leq \Delta L_{i,t}^j \leq (D_{i,t}^j - D_{i,t}^{j-1}), j = 2, 3, \dots, J \quad (8)$$

$$\Delta L_{IB,t} = \sum_{i=1}^I \sum_{j=1}^J \Delta L_{i,t}^j \tag{9}$$

where ΔL_i is actual load reduction, t is the time and j is the step, D_i is available load reduction, and ΔL_{IB} is the output power provided by IBDR.

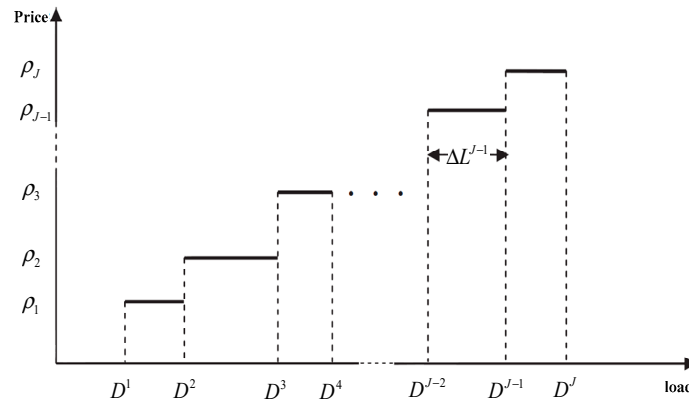


Figure 2. Gradual price and demand curve for Demand Response (DR).

2.3. Heating Output Model

The main heating output sources of the HES are CHP and RE. CHP also provides electric power and heating power. Although CHP is the component that couples the electric and heating power systems, in this work, CHP is regarded as a heating source.

2.3.1. CHP Output Model

The heating power provided by CHP determines the interval threshold of its electricity power supply. In general, CHP can be categorized as either backpressure type or exhaust-pressure type. This paper mainly discusses the exhaust-pressure type of CHP with emphasis on the constraint on electricity power and heating power [6]. Figure 3 shows the relationship between electric power and heating power of the CHP.

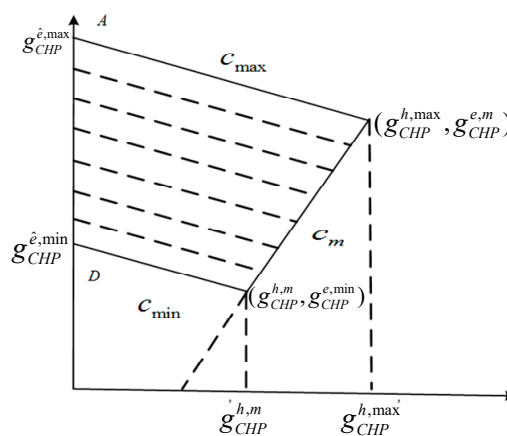


Figure 3. Electric power and heating power curve.

The paper mainly consider the constraints of CHP in power generation and heating supply as shown follows:

$$0 \leq g_{CHP,t}^h \leq g_{CHP,t}^{h,max} \tag{10}$$

$$g_{CHP,t}^e \leq g_{CHP}^{e,max} + c_{max} g_{CHP,t}^h \tag{11}$$

$$g_{CHP,t}^e \geq g_{CHP}^{e,\min} + c_{\min} g_{CHP,t}^h \quad (12)$$

$$g_{CHP,t}^e \geq g_{CHP,t}^{e,\min} + c_m \left(g_{CHP,t}^h - g_{CHP,t}^{h,m} \right) \quad (13)$$

where $g_{CHP,t}^h$ and $g_{CHP,t}^e$ are the supply of heating power and electricity power of CHP at time t , and $g_{CHP}^{h,\max}$ is the maximum heating power supply. Here, $g_{CHP}^{e,\min}$ and $g_{CHP}^{e,\max}$ are the maximum and minimum values of CHP power supply under pure condensation conditions, and $g_{CHP}^{e,\min}$ is the minimum heating power of CHP corresponding to the minimum electricity power. Also, c_{\max} and c_{\min} are the linear supply slopes of heating power and electric power of CHP, while $g_{CHP}^{e,\min}$ is the minimum electricity power of CHP, and $g_{CHP}^{h,m}$ is the heating power of CHP when the electric power reaches the minimum value.

2.3.2. RE Output Model

RE includes RE-EB and RE-HS modules. During peak load of WT and PV generation, RE-HS can convert surplus electric energy into heating energy, further enhancing the space for energy management system (EMS) to absorb WT and PV. The heating energy generated by RE is stored in a hot water tank as a heating accumulator which uses water as the heating medium.

(1) RE-EB operation model

RE-EB is based on a coupling unit of energy conversion, relying on electrical elements to achieve heating purposes. If the heating energy generated by RE-EB comes from waste energy, the local electricity load will relatively increase. The detailed model is expressed as:

$$Q_{EB,t}^{RE} = g_{EB,t}^{RE} \cdot \eta_{EB,t}^{RE} \quad (14)$$

where g_{EB}^{RE} is the electric power for the heating supply of RE-EB, Q_{EB}^{RE} means the heating power supply of RE-EB, and η_{EB}^{RE} means the efficiency of thermal–electrical conversion.

(2) RE-HS operation model

When RE is installed with a heating storage device, heating storage can be performed using waste energy when the WT and PV power output are high. Then, the heat can be released during the peak load period of heating energy demand:

$$S_{HS,t}^{RE} = (1 - \varphi_{HS}) S_{HS,t-1}^{RE} + \left(Q_{HS,t}^{RE} \eta_{HS}^{in} - \frac{Q_{HS,t}^{out}}{\eta_{HS}^{out}} \right) \quad (15)$$

where S_{HS}^{RE} is the storage capacity for RE-HS, φ_{HS} is the heat dissipation loss rate of HS, Q_{HS}^{RE} is the heating power used for RE-HS, and the calculation method is the same as Equation (14). Here, Q_{HS}^{out} is the exothermic power for RE-HS, and η_{HS}^{in} and η_{HS}^{out} are the endothermic and exothermic efficiency, respectively.

3. Multi-Objective Scheduling Optimization Model

3.1. Objective Functions

The purpose of HES optimization scheduling is to meet the power and heating load requirements combined with CGT and CHP by enhancing the connection between WT and PV and the grid. Since WT and PV are environmentally friendly and their marginal power generation costs are very small, the maximum economic benefit can be obtained by maximizing the power output of both. However, the randomness of WT and PV brings a high risk of unstable system operation. How to minimize the operational risk while maximizing revenue is the key issue of HES operation. Therefore, in this work,

we chose the maximum economic revenue and the minimum risk level as the objective functions of HES optimization operation.

3.1.1. The Maximum Operation Revenue Objective

The net revenue of HES operation mainly depends on two factors: revenue and cost. HES operation revenue comes from WT, PV, CGT, IBDR, CHP, and RE, while the operating costs of HES consist of four parts, the operating costs of CGT, CHP and RE, and the cost of buying electricity from the public grid. We use the maximum operating income as the objective function:

$$\max F_1 = \sum_{t=1}^T \{R_{WPP,t} + R_{PV,t} + R_{CGT,t} + R_{IBDR,t} + R_{CHP,t} + R_{RE,t} - \rho_{UG,t}g_{UG,t}\} \quad (16)$$

where F_1 is the objective function of HES operation net revenue; R is the operating income. ρ is the price of buying electricity from the grid, g is the amount of electricity purchased. The revenue models of the above components are calculated as follows:

$$R_{CGT,t} = \rho_{CGT,t}g_{CGT,t} - C_{CGT,t}^{pg} - C_{CGT,t}^{ss} \quad (17)$$

$$C_{CGT,t}^{pg} = a_{CGT} + b_{CGT}g_{CGT} + c_{CGT}(g_{CGT,t})^2 \quad (18)$$

$$C_{CGT,t}^{ss} = [u_{CGT,t}(1 - u_{CGT,t-1})] \cdot \begin{cases} N_{CGT}^{hot}, T_{CGT}^{min} < T_{CGT,t}^{off} \leq T_{CGT}^{min} + T_{CGT}^{cold} \\ N_{CGT}^{cold}, T_{CGT,t}^{off} > T_{CGT}^{min} + T_{CGT}^{cold} \end{cases} \quad (19)$$

where C is the cost of power generation; pg means start and ss means close; t is the time, and a , b , and c are the cost coefficients. Here, g is the power output; u is the operation status, a binary variable. Also, N_{CGT}^{hot} and N_{CGT}^{cold} are the CGT cold and hot startup costs, respectively; while T is the operating time.

$$R_{IBDR,t} = \sum_{i=1}^I \sum_{j=1}^J \Delta L_{i,t}^j \rho_{i,t}^j \quad (20)$$

where ρ is the output price, j is the step and t is the time. Moreover, CHP's operating income is calculated by the following formula:

$$R_{CHP,t} = \sum_{t=1}^T \left\{ \left(\rho_{CHP,t}^e g_{CHP,t}^e + \rho_{CHP,t}^h g_{CHP,t}^h \right) - \left(f(g_{CHP,t}) + C_{CHP,t}^{sd} \right) \right\} \quad (21)$$

$$f(g_{CHP,t}) = a_i \left(g_{CHP,t}^e + \theta_h^e g_{CHP,t}^h \right)^2 + b_i \left(g_{CHP,t}^e + \theta_h^e g_{CHP,t}^h \right) + c_i \quad (22)$$

$$C_{CHP,t}^{sd} = [\mu_{CHP,t}^u(1 - \mu_{CHP,t-1}^u)] C_{CHP,t}^u + [\mu_{CHP,s}^d(1 - \mu_{CHP,s+1}^d)] C_{CHP,s+1}^d \quad (23)$$

where f is the cost function and C is the cost of power generation, sd means startup–shutdown. Here, t and s are the indexes for time, $t \neq s$; ρ is the grid-prices and e means power, h means heating; g is the output; and a , b , and c are the cost coefficients. Also, θ_h^e is the thermal–electricity conversion coefficient of CHP; μ is the operation status, 0–1 variables:

$$R_{RE,t} = \sum_{t=1}^T \left(\rho_{RE,t}^h Q_{RE,t} - \rho_{RE,t}^e g_{RE,t} \right) \quad (24)$$

where t is the time; ρ_{RE}^e is the prices for power and ρ_{RE}^h the prices for heating; Q_{RE} is the heating output of RE; and g_{RE} is the power input of RE.

3.1.2. The Minimum Load Fluctuation Objective

Large-scale integration of WT and PV into the grid will bring high risk of unstable system operation because their power output is intermittent and volatile. Thus, reasonable control of this HES operation risk is essential. In this work, the net load fluctuation was chosen as the risk index, and the objective function selects the minimum load fluctuation and represent it by the following formula:

$$\min F_2 = \left\{ \sum_{t=1}^T \left[g_{WPP,t} + g_{PV,t} - \left(\Delta L_{IB,t}^- - \Delta L_{IB,t}^+ \right) - \left(Q_{HS,t}^{out} - Q_{HS,t}^{RE} \right) / \eta_{HS}^{in} - \bar{g}_{VPP} \right]^2 / T \right\}^{1/2} \quad (25)$$

$$\bar{g}_{VPP} = \sum_{t=1}^T \left[g_{WPP,t} + g_{PV,t} - \left(\Delta L_{IB,t}^- - \Delta L_{IB,t}^+ \right) - \left(Q_{HS,t}^{out} - Q_{HS,t}^{RE} \right) / \eta_{HS}^{in} \right] / T \quad (26)$$

where F_2 is the objective of HES load fluctuation, $\bar{g}_{VPP,t}$ is the average load fluctuation for the HES throughout the entire scheduling period, t is the time. The $\left(\Delta L_{IB,t}^- - \Delta L_{IB,t}^+ \right)$ is the net output of IBDR.

3.2. Constraint Conditions

For HES operations, three constraints are considered, supply and demand balance constraints, energy operation constraints, and system reserve constraints.

3.2.1. Energy Balance Constraints

(1) Electricity Balance Constraints

$$\underbrace{\left\{ g_{WPP,t}^e (1 - \varphi_{WPP}) + g_{PV,t}^e (1 - \varphi_{PV}) + g_{CHP,t}^e (1 - \varphi_{CHP}) + u_{IB,t} \Delta L_{IB,t}^E - \left(g_{EB,t}^{RE} + g_{HS,t}^{RE} \right) \right\}}_{\text{MES Power output in day ahead scheduling}} + g_{UG,t} \geq L_t^0 - u_{PB,t}^e \Delta L_{PB,t} \quad (27)$$

where φ_{WPP} , φ_{PV} , and φ_{CHP} are the power loss rates. Here, $g_{UG,t}$ is the electricity purchased from the grid; L_t^0 is the load required by the end user; and $g_{EB,t}^{RE}$ is the input electricity of RE-EB and $g_{HS,t}^{RE}$ is the input electricity of RE-HS. Also, μ_{IB} is the status variables of IBDR and μ_{PB} is the status variables of PBDR, binary variables. Use 1 and 0 to indicate whether DR is implemented, where 1 is the implementation and 0 is not implemented. Use ΔL to indicate the amount of change in load. According to microeconomic theory, PBDR can also be described by demand and price, as follows:

$$e_{st} = \frac{\Delta L_s / L_s^0}{\Delta P_t / P_t^0} \begin{cases} e_{st} \leq 0, s = t \\ e_{st} \geq 0, s \neq t \end{cases} \quad (28)$$

where Δ represents the amount of change after adding PBDR, L is the demand, P is the price. Then, calculate the load change after adding PBDR by the following formula:

$$\Delta L_{PB,t} = L_t^0 \times \left\{ e_{tt} \times \frac{[P_t - P_t^0]}{P_t^0} + \sum_{\substack{s=1 \\ s \neq t}}^{24} e_{st} \times \frac{[P_s - P_s^0]}{P_s^0} \right\} \quad (29)$$

where L_t^0 is the load demand before PBDR and L_t is the load demand after PBDR; P_t^0 is the electricity price before PBDR and P_t is the electricity price after PBDR; and e_{st} represents the elasticity of price and demand. If $s = t$ then e_{st} is called self-elasticity, if $s \neq t$ then e_{st} is called cross-elasticity. [8] gave a detailed mathematical description of the above relationship.

(2) Heating balance constraints

$$g_{CHP,t}^h + Q_{EB,t}^{RE} + Q_{HS,t}^{out} = Q_t - u_{PB,t}^h \Delta Q_t \quad (30)$$

where Q is the heating demand of terminal customers, Q^{out} is the heating output, and u_{PB}^h is the status variable of implementing PBDR for the heating load, a binary variable. Use 1 and 0 to indicate whether PBDR is implemented, where 1 is the implementation and 0 is not implemented. ΔQ indicates the amount of load change before and after adding PBDR. The detailed calculations are the same as Equations (28) and (29). The constraints for the load of power and heating produced by PBDR are given in [8].

3.2.2. Power Source Operation Constraints

(1) CGT operation constraints

The constraints of the conventional turbine generation (CTG) operation consist of three parts, the operation constraint, the climb constraint, and the start closure constraint, which can be expressed as follows:

$$u_{CGT,t} g_{CGT}^{\min} \leq g_{CGT,t} \leq u_{CGT,t} g_{CGT}^{\max} \quad (31)$$

$$u_{CGT,t} \Delta g_{CGT}^- \leq g_{CGT,t} - g_{CGT,t-1} \leq u_{CGT,t} \Delta g_{CGT}^+ \quad (32)$$

$$(T_{CGT,t-1}^{\text{on}} - M_{CGT}^{\text{on}})(u_{CGT,t-1} - u_{CGT,t}) \geq 0 \quad (33)$$

$$(T_{CGT,t-1}^{\text{off}} - M_{CGT}^{\text{off}})(u_{CGT,t} - u_{CGT,t-1}) \geq 0 \quad (34)$$

where g_{CGT}^{\min} and Δg_{CGT}^+ is the upper limits of CGT, and g_{CGT}^{\max} and Δg_{CGT}^- is the lower limits of CGT, T is the duration time, M is the shortest time, on stands for running or power on, and off stands for downtime.

(2) IBDR constraints

IBDR can be used to schedule energy and reserve markets. Specific restrictions are expressed by the following formula:

$$\Delta L_{IB,t}^E + \Delta L_{IB,t}^{up} \leq \Delta L_{IB,t}^{\max} \quad (35)$$

$$\Delta L_{IB,t}^E + \Delta L_{IB,t}^{dn} \geq \Delta L_{IB,t}^{\min} \quad (36)$$

where ΔL dicates the amount of change in scheduling capability after joining IBDR, t means time and E means load; ΔL_{IB}^{up} and ΔL_{IB}^{dn} are the maximum and minimum reserve outputs of IBDR in the reserve market; ΔL_{IB}^{\max} and ΔL_{IB}^{\min} are the maximum and minimum output of IBDR. The IBDR should also consider the upper and lower reserve capacities of the heat load. The specific formula is as follows:

$$u_{IB,t} \Delta L_{IB}^- \leq \Delta L_{IB,t} - \Delta L_{IB,t-1} \leq u_{IB,t} \Delta L_{IB}^+ \quad (37)$$

$$(T_{IB,t-1}^{\text{on}} - M_{IB}^{\text{on}})(u_{IB,t-1} - u_{IB,t}) \geq 0 \quad (38)$$

$$(T_{IB,t-1}^{\text{off}} - M_{IB}^{\text{off}})(u_{IB,t} - u_{IB,t-1}) \geq 0 \quad (39)$$

where $+$ represents the upper limit $-$ represents the lower limit; T represents the continuous time and M represents the shortest time, and on is the operating state off is the stop state.

(3) WT and PV Operation constraints

$$0 \leq g_{NE,t} \leq g_{NE,t}^*, \{NE\} = \{WPP, PV\} \quad (40)$$

where g_{NE} is the output of NE , and g_{NE}^* means the revised output of NE .

3.2.3. Heating Power Operation Constraints

(1) CHP operation constraints

Changes in the CHP output should be realized by changing the operation state of the boiler. Therefore, the power output should be converted by combing power and heating under the working condition of a pure condensing condition for constructing the climbing output constraint. The detailed conversion process is expressed as:

$$g_{CHP,t} = g_{CHP,t}^e + \theta_h^e g_{CHP,t}^h \quad (41)$$

where g_{CHP} is the output of CHP under the working condition of the pure condensing condition. CGT and CHP operation also must meet the upper and lower climbing constraints, startup–shutdown time constraints, and power output constraints. The detailed constraints are the same as Equations (31)–(34).

(2) RE operation constraints

There are three main types of RE operating restrictions: electric boiler operating constraints, HS operating constraints and energy balance constraints, which are expressed as follows:

$$0 \leq Q_{EB,t}^{RE} + Q_{HS,t}^{out} \leq Q_{RE,t}^{max} \quad (42)$$

$$S_{HS,T}^{RE} = S_{HS,0}^{RE} \quad (43)$$

$$S_{HS}^{RE,min} \leq S_{HS,t}^{RE} \leq S_{HS}^{RE,max} \quad (44)$$

$$0 \leq Q_{HS,t}^{out} \leq \eta_{HS}^{out} Q_{HS,nom} \quad (45)$$

$$0 \leq Q_{HS,t}^{RE} \leq \eta_{HS}^{in} Q_{HS,nom} \quad (46)$$

$$Q_{HS,t}^{out}, Q_{HS,t}^{RE} = 0 \quad (47)$$

where Q_{RE}^{max} represents the maximum output of RE; $S_{HS,0}^{RE}$ and $S_{HS,T}^{RE}$ represent the storage heating by the HS at the beginning and end of the schedule, respectively; $S_{HS}^{RE,min}$ and $S_{HS}^{RE,max}$ represent the minimum and maximum capacities of HS under stable operation condition, respectively. $Q_{HS,nom}$ is the rated capacity of HS.

3.2.4. System Reserve Constraints

Fluctuations in WT and PV output can affect the stability of HES operation, so by preserving the corresponding power to overcome the impact, the corresponding power capacity should be reserved, and the constraints are expressed in detail as:

$$g_{EMS,t}^{e,max} - g_{EMS,t}^e + \Delta L_{IB,t}^{up} \geq r_1 L_t + r_2 g_{WPP,t} + r_3 g_{PV,t} \quad (48)$$

$$g_{EMS,t}^e - g_{EMS,t}^{e,min} + \Delta L_{IB,t}^{dn} \geq r_4 g_{WPP,t} + r_5 g_{PV,t} \quad (49)$$

where g_{MES}^{max} and g_{MES}^{min} represent the maximum and minimum values of the HES output, respectively; g_{VPP} represents the output of HES; r_1 , r_2 , and r_3 represent the upper reserve factors of power load, WT, and PV, respectively; r_4 and r_5 represent the lower reserve factors of WT and PV, respectively. Similarly, the upper and lower reserve capacities for the heating load should be considered. The constraints are expressed in detail as:

$$\left(g_{CHP,t}^{h,max} - g_{CHP,t}^h \right) + \left(Q_{RE,t}^{max} - Q_{HS,t}^{RE} - Q_{EB,t}^{out} \right) \geq r_6 Q_t \quad (50)$$

$$\left(g_{CHP,t}^h - g_{CHP,t}^{h,min} \right) + \max \left\{ Q_{HS,t}^{out}, S_{HS}^{RE,max} - S_{HS,t}^{RE} \right\} \geq r_7 Q_t \quad (51)$$

where r_6 and r_7 are the upper and lower reserve coefficients of the heating load.

4. Solution Methodology for Multi-Objective Model

4.1. Linearization

4.1.1. Linearization of Objective Functions

According to Equations (18), (20), and (22), there are many functions with quadratic terms in the objective function F_1 . Therefore, to simplify the solution process, we handle them with the following method. Taking Equation (18) as an example, the CGT's output limitation $[g_{CGT,t}^{\min}, g_{CGT,t}^{\max}]$ is divided into N segments. The length of each segment is Δg_{CGT} , so the segmentation function can be represented by F_1 when $g_{CGT,t} \in [g_{CGT,t}^{\min} + n\Delta g_{CGT}, g_{CGT,t}^{\min} + (n+1)\Delta g_{CGT}]$:

$$f'(g_{CGT,t}) = f'(g_{CGT}^{\min} + n\Delta g_{CGT}) + (g_{CGT,t} - g_{CGT}^{\min} - n\Delta g_{CGT}) \times [b_{CGT} + (2n+1)c_{CGT} \cdot \Delta g_{CGT} + 2c_{CGT}g_{CGT}^{\min}] \quad (52)$$

Here, $n = 0, 1, \dots, N-1$ and $\Delta g_{CGT} = (g_{CGT}^{\max} - g_{CGT}^{\min})/N$. Similarly, the output of other quadratic terms is the same as Equation (18). When $N \geq 5$, the relative error of the objective function does not exceed 1%, and most of it is below 0.5%. The approximation error of the segmented figure is close to 0. Figure 4 shows the objective function linearization process.

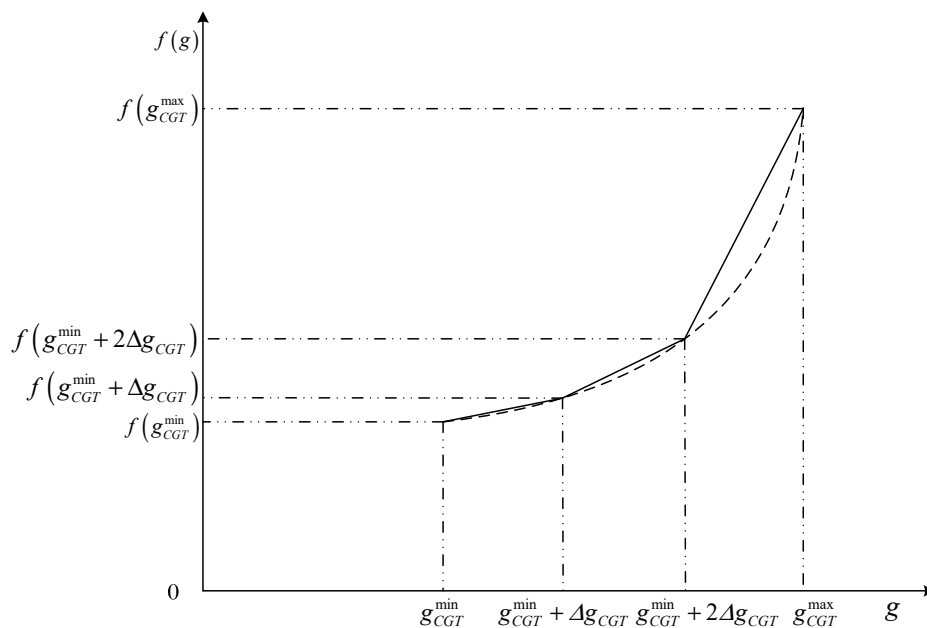


Figure 4. Objective functions' linearization process.

4.1.2. Linearization of Constraint Conditions

According to Equations (33), (34), (38), and (39), there are also functions with quadratic terms in the constraints, which also must be linearized. Similarly, taking CGTs as an example, the linearization progress of constraint conditions is carried out as follows:

- (1) Initial status constraints

$$\sum_{t=1}^L (1 - u_{i,t}) = 0 \quad (53)$$

$$\sum_{t=1}^D (u_{i,t}) = 0 \quad (54)$$

where L is the number of CGTs in the initial status. $L = 0$ is no initial state. Here, M indicates the number of CGTs that are not in the initial state, and U^0 is the time period of CGT operation at the start of the scheduling period. Then L can be calculated as:

$$L = \min\left\{T, \left(M_{CGT}^{on} - U^0\right)u_{CGT,t}\right\} \quad (55)$$

$$M = \min\left\{T, M_{CGT}^{off}(1 - u_{CGT,t})\right\} \quad (56)$$

(2) Startup–shutdown constraints

$$\sum_{\tau=t}^{T_1} u_{CGT,t} \geq T_{CGT,t}^{on} M_{CGT}^{on}, T_1 = t + M_{CGT}^{on} - 1, \forall t = L + 1, \dots, T - M_{CGT}^{on} + 1 \quad (57)$$

$$\sum_{\tau=t}^{T_2} [1 - u_{CGT,t}] \geq T_{CGT,t}^{off} M_{CGT}^{off}, T_2 = t + M_{CGT}^{off} - 1, \forall t = D + 1, \dots, T - M_{CGT}^{off} + 1 \quad (58)$$

$$\sum_{\tau=t}^T [u_{CGT,t} - T_{CGT,t}^{on}] \geq 0 \forall t = T - M_{CGT}^{off} + 2, \dots, T \quad (59)$$

$$\sum_{\tau=t}^T [1 - u_{CGT,t} - T_{CGT,t}^{off}] \geq 0 \forall t = T - M_{CGT}^{off} + 2, \dots, T \quad (60)$$

4.2. Comprehensive Objective Function

HES optimization scheduling model proposed by the two objective functions consisting of maximum economic return and minimum load fluctuation. In general, high system operating income will result in relatively high load fluctuations in HES output. Different weights are usually set for each target to achieve an optimization scheme, for example, by setting different weights to convert multi-target HES into single-target HES. Therefore, the operation optimization problem of HES can be divided into three stages. First, the biggest economic gain is the optimization goal, the optimal value of HES economical revenue F_1^{\max} and the output fluctuation F_{12} are obtained. Second, the minimum output fluctuation is the optimization goal, the minimum value of the output fluctuation F_2^{\min} and the economical revenue F_{21} are obtained. Third, due to the differences in the optimization directions of the objective function, the weight coefficients of the objective functions are set as α_1 and α_2 , Where α_1 is the weighting factor of the largest economic income, and α_2 is the weighting factor of the minimum output fluctuation. The two objective functions are combined into one objective function by weighting them. The weight objective function is:

$$F = \min\left\{\alpha_1 \cdot \frac{F_1^{\max} - F_1}{F_1^{\max}} + \alpha_2 \cdot \frac{F_2 - F_2^{\min}}{F_2^{\min}}\right\} \quad (61)$$

where $\alpha_1 + \alpha_2 = 1$; if α_1 and α_2 are set, the optimal F_1 and F_2 can be achieved. Figure 5 shows a flow chart of the HES scheduling optimization model.

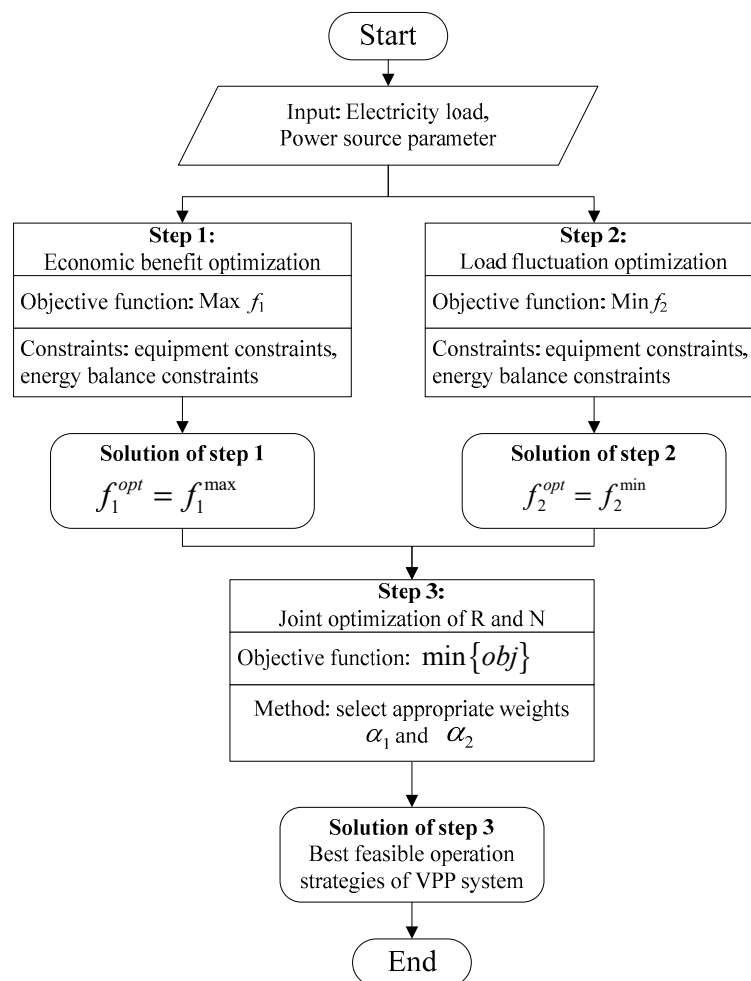


Figure 5. Flow chart of HES scheduling optimization model.

5. HES Simulation Scenarios

Case 1: The fundamental scenario, HES has on RE-HS or PBDR self-scheduling. This scenario is used as a reference scenario mainly to determine the optimal weight coefficient of the objective function. This case is mainly used for comparatively analyzing the improvement effect of RE-HS and PBDR on clean energy for HES operation.

Case 2: The PBDR scenario, HES only uses PBDR for self-scheduling. Comparing this situation with *Case 1*, we can determine the optimization results of PBDR for HES operation. PBDR can use the time-of use (TOU) price to optimize the load distribution, which influences the operation plan of different HES components. The flattening effect of PBDR on the load demand curve is analyzed.

Case 3: The RE-HS scenario, HES only uses RE-HS for self-scheduling. Unlike *Case 1*, this case considers the status of HES operation with RE-HS. RE changes the basic operation mode of WT and PV only satisfying the load demand of power electricity, and transform the remaining wind and solar energy into heating energy. RE-HS can also use the energy stored in the load valley for the load peak, which also flattens the heating demand curve.

Case 4: Integrated programs, HES use RE-HS and PBDR for self-scheduling. Based on *Case 2* and *Case 3*, this case is used to determine the optimal scheduling strategy of HES operation and analyzes the synergistic optimization effect when RE and PBDR are simultaneously applied.

6. Simulation Analysis

6.1. Basic Data

The selected simulation system is a microgrid on an island located in eastern China. The proposed multi-objective optimal scheduling model is validated and verified whether the proposed algorithm is effective and applicable [30]. The micro-grid comprises $2 \times 0.5 \times 10^3$ kW WTs, $5 \times 0.2 \times 10^3$ kW PV plants, $1 \times 1.5 \times 10^3$ kW CGTs, $1 \times 0.5 \times 10^3$ kW RE boilers with a 5×10^3 kWh energy storage system, and 1 CHP with the maximum heating output of 1.44×10^3 kW and maximum power output of 1.2×10^3 kW. The thermoelectric output ratio of CHP is 1.2, and other operating parameters were adopted according to [30]. The CGT units are diesel generators. The rate of rise is 0.1×10^3 kWh rate at which 0.2×10^3 kWh decreases. It takes 0.2 hours to start the machine and 0.1 hours to shut down the machine. It takes 0.102 ¥/kW h to start and shut down. In [8], divides the cost curve into two linearized segments of different slopes with slopes 1.1×10^5 ¥/ kW and 3.62×10^5 ¥/ kW, respectively. To facilitate the calculation, set all of the reserve coefficients as 0.05. Furthermore, based on historical data of electricity load and heating load, the demand load distribution for power and heating on a typical load day is predicted using an autoregressive moving average model (ARMA). Figure 6 is the demand load distribution of electricity and heating in typical daily load.

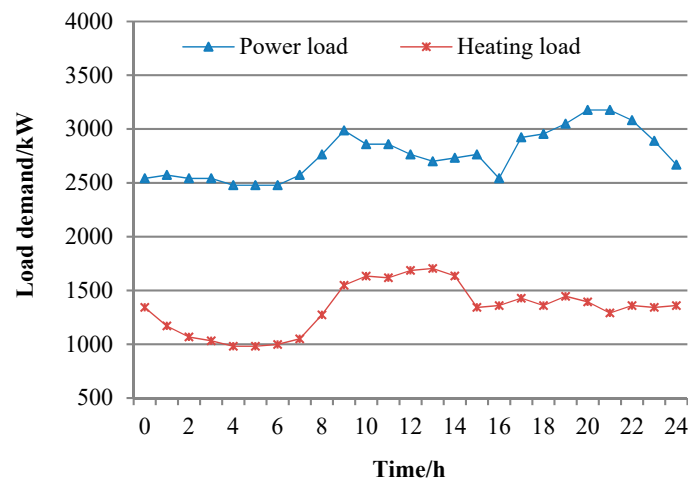


Figure 6. Demand load distribution of electricity and heating in typical daily load.

For power supply, the grid-connected electricity price of CGT, WT, PV are 0.57 ¥/kWh, 0.85 ¥/kWh and 0.52 ¥/kWh in the micro-grid, respectively. According to [30], the parameters of WT are $v_{in} = 3$ m/s, $v_{rated} = 14$ m/s, $v_{out} = 25$ m/s, and φ is a shape parameter, its value is 2; θ is a proportional parameter, and its value is $2v/\sqrt{\pi}$. The illumination intensity parameter α is equal to 0.39, β equal to 8.54. We simulate the output of the WT and PV using the method proposed in [31], and a total of 50 different simulation scenarios were thus obtained. After that, use some measures to reduce 50 simulated scenes to 10 typical scenes, as shown in [8]. Input data is the average of all scenarios. Figure 7 is the typical scene set for WT and PV simulation.

As shown in Figure 6, the load can be divided into three time periods: peak period (9:00–11:00 and 18:00–24:00), floating period (12:00–17:00) and valley period (0:00–8:00). Comparing the price of electricity before and after PBDR application, before the application, the power consumption price is 0.55 ¥/kWh. After the application, the electricity price of the three time periods has changed, the peak price has increased by 25%, and the floating period remains unchanged. The valley period has dropped by 50%. The load change caused by adding PBDR is limited to 0.4×10^3 kW below. The prices for participating in the reserve are 0.65 ¥/kWh and 0.25 ¥/kW h, respectively.

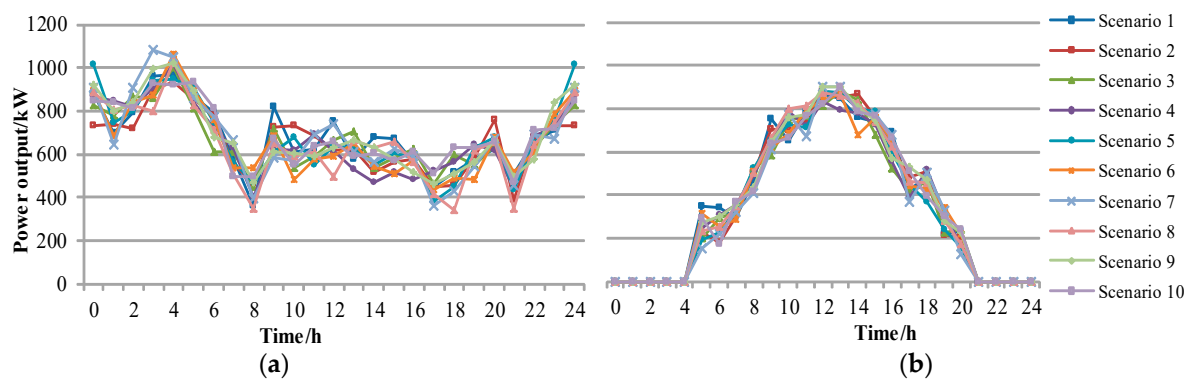


Figure 7. Typical simulation scenarios of wind turbine (WT)(a) and photovoltaic (PV)(b).

For heating supply, the marginal cost of wind and photovoltaic power generation is almost zero or even negative, a preferential electricity price of 0.1 ¥/kWh is given to encourage RE to use waste energy to provide heating at nighttime. The electric power supply price of CHP is the same as that of CGT, and the heating power supply price is 0.25 ¥/kWh. Since there have been few studies related to the price elasticity of heating demand, this paper mainly discuss the optimal operation of PBDR in relation to heating load for HES operation. Therefore, according to the change of electricity price, the heating price of three different load periods is set, in which the peak period rises by 25%, the floating period remains unchanged, and the valley period drops by 50%. Depending on the heating price, the load in the three periods also changed, with a peak period of 15%, a floating period of 5%, and a valley period of 15%. All the load changes follow proportional allocation at each time. Figure 7 shows the system wind power output levels at different P2G equipment capacities. In addition, P2G equipment can improve the integration of renewable energy in the electric-gas-heat combination system and reduce system energy consumption and reduce system carbon emissions. P2G equipment converts surplus wind power into natural gas, and generates electricity from local CHP at the peak of power load, which reduces the natural gas and electricity that the energy center obtains from the network, thereby reducing the transmission loss and the ratio of the gas used by the pressurized station to the total gas consumption. CHP can reduce the natural gas and electricity that the energy center obtains from the network, thereby reducing the transmission loss and the ratio of the gas used by the pressurized station to the total gas consumption. We input the above basic data and solve the proposed four models using GAMS software described in [31].

6.2. Scheduling Operation Results

6.2.1. Self-Scheduling of HES Operation in Case 1

Case 1 is mainly used as a reference scenario for analyzing the optimizing effects of RE-HS and PBDR on HES operation. When HES operates without RE, heating energy is mainly supplied by CHP. Under the FTL mode, the power generated by CHP contributes to the power coordination optimization for HES operation scheduling. Table 1 shows the scheduling results of HES operation for different objective functions.

Table 1. Scheduling results of hybrid energy system (HES) operation for different objective functions.

Objective	Objective Value		CGT	WT	PV	IBDR	CHP		RE-EB	Waste Energy	
	F1/¥	F2/ $\times 10^3$ kW					Power	Heating		WT	PV
F1	50837.03	0.275	26.61	11.13	5.39	3.285	25.857	31.028	2.54	4.835	3.31
F2	49852.45	0.246	36.90	3.71	2.11	3.435	26.132	31.358	2.21	12.25	6.60

According to Table 1, the HES makes full use of WT and PV to obtain higher economic benefits under the maximum operation revenue mode (mode 1), but a higher grid connection ratio of WT and PV also causes higher load fluctuations. Compared with the minimum load fluctuation mode (mode 2), HES operation revenue increases 984.58 ¥, and the energy wasted by WT and PV reduces 7.421×10^3 kWh and 3.287×10^3 kWh, respectively, but the load fluctuation increases by 0.029×10^3 kW. On the other hand, the heating supply of RE decreases from 2.545×10^3 kWh to 2.215×10^3 kWh in mode 1; however, the value decreases 0.33×10^3 h in mode 2. In general, mode 1 follows the maximum operation economic revenue, while mode 2 follows the minimum operational risks, so it is necessary to consider how to balance the two modes. Then, to determine the optimal weight coefficient, sensitivity analysis of the weighting coefficients of the objective function. The weight of F_1 is gradually increased from 0.1 to 1, and the interval is 0.1 each time. The HES scheduling results under various weighted combination schemes are obtained. Figure 8 shows the objective function values under various weight coefficients.

As seen in Figure 8a, when $\alpha_1 = 1$ and $\alpha_2 = 0$, the revenue of HES operation reaches the optimal value (F_1^{\max}), and when $\alpha_2 = 1$ and $\alpha_1 = 0$, the load fluctuation of HES operation reaches the optimal value (F_2^{\min}). Then, the trend of F_1 and F_2 is analyzed in relation to changes in α_1 . When $\alpha_1 \in [0, 0.2]$ and $\alpha_1 \in [0.7, 0.9]$, the objective function value rises especially quickly because, in the actual operation, the maximum economic benefits meet the demands of the decision makers. When $\alpha_1 \in [0, 0.2]$, the revenue is lower than that when $\alpha_1 \in [0.7, 0.9]$, therefore, the optimal weight coefficients should be distributed when $\alpha_1 \in [0.7, 0.9]$.

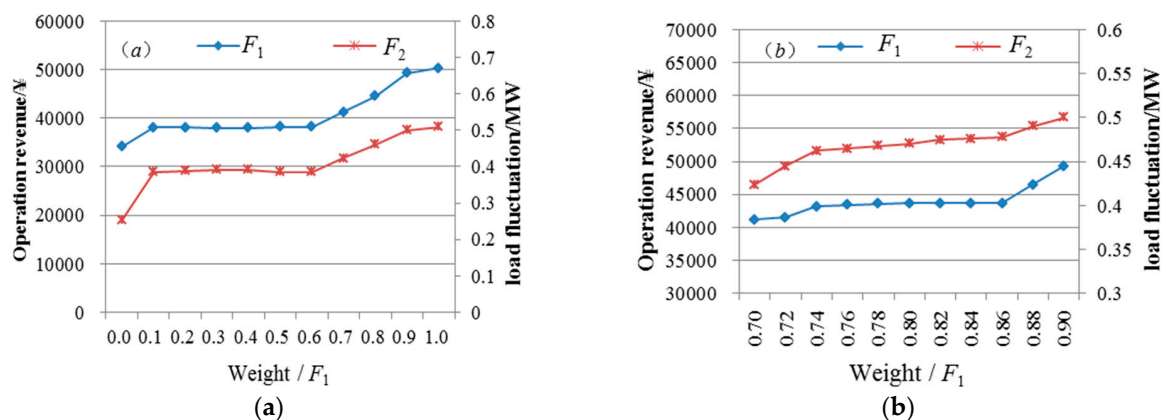


Figure 8. Objective function values under $\alpha_1 \in [0, 0.2]$ (a) and $\alpha_1 \in [0.7, 0.9]$ (b).

As seen in Figure 8b, when $\alpha_1 \in [0.74, 0.86]$, the revenue and load fluctuation of HES operation basically become stable, that is, HES operation reaches an overall optimum. When $\alpha_1 \notin [0.74, 0.86]$, the objective value of ESM operation varies widely, which indicates that HES can be continually optimized. Therefore, we selected $\alpha_1 \in [0.74, 0.86]$ as the optimal weight coefficients and set the weight of the objective function as $\alpha_1 = 0.78$ and $\alpha_2 = 0.22$. Then, the optimal results of HES operation could be obtained under the weighted signal objective function. Obviously, decision makers can adjust the weight of the objective function according to their own actual situations. In general, when decision makers are more sensitive to risk, they will set a relatively large α_2 . Figure 9 shows the scheduling results of HES operation for Case 1.

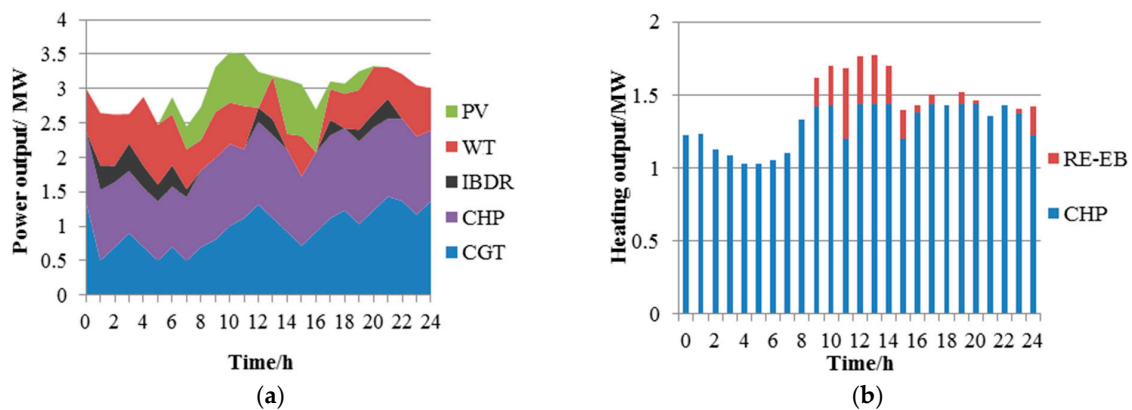


Figure 9. The results of HES operation after application of PBDR (a) and RE-HS (b) for *Case 1*.

According to the weights shown in Figure 8, the scheduling results of HES operation in *Case 1* can be obtained. The revenue value and load fluctuation are 50337.03 ¥ and 0.253×10^3 kW, respectively. In terms of power supply, WT, PV, and CHP are high-priority to provide power. CGT can quickly start and stop; therefore, CGT is scheduled more during the peak load periods. During the valley load and float load periods, IBDR is scheduled because the power output of PV is low. In terms of heating supply, CHP is preferentially scheduled to meet heating demand, in order to meet the remaining heating energy demand, RE is scheduled during peak load. The output of WT is 13.575×10^3 kWh waste energy is 2.395×10^3 kWh, and the output of PV is 6.417×10^3 kWh waste energy is 2.293×10^3 kWh. In general, since RE does not install heating storage devices in this case, the power generated by WT and PV can hardly be stored during the peak load periods. Further utilization of WT and PV should be studied. Meanwhile, if PBDR can be used to flatten the load demand curve and increase the demand for load in the valley period, it may also increase the grid connection space of WT and PV.

6.2.2. Self-Scheduling of HES Operation in *Case 2*

Case 2 can analyze the effects of adding PBDR to HES operations. We join the PBDR and balance the power load demand curve with the TOU price. Referring to the weight calculation method in *Case 1*, in *Case 2*, the weight coefficients of F1 and F2 were set as 0.72 and 0.28, respectively. Then get the optimal scheduling result of HES operation after joining PBDR. First, the load demand curve of power and heating after application of PBDR were determined. Table 2 shows the load demand changes added to the PBDR.

Table 2. Load demand changes added to the price-based demand response (PBDR).

Scenario	Power Load $\times 10^3$ kW			Heating Load $\times 10^3$ kW			Peak–Valley Ratio	
	Peak	Float	Valley	Peak	Float	Valley	Power	Heating
Before PBDR	24.141	24.522	20.425	11.646	13.198	8.551	1.282	1.737
After PBDR	23.176	24.414	20.833	11.180	13.149	8.722	1.207	1.703
Difference	−0.966	−0.108	0.408	−0.466	−0.049	0.171	−0.075	−0.034

As shown in Table 2, the power load requirements of the three periods after the addition of PBDR have changed, with the peak period decreasing, the valley period increasing, and the floating period being appropriately reduced, which leads to a significant peak-shaving and valley-filling effect. Regarding the power load, the total demand decreases 0.966×10^3 kWh during the peak periods, whereas the value increases 0.408×10^3 kWh during the valley period, peak to valley ratio decreased by 0.075. Similarly, regarding the heating load, peak to valley ratio decreased by 0.034. All in all, by increasing PBDR, not only can the load demand curve be balanced, but also the grid connection space between WT and PV can be increased. Figure 10 shows the results of HES scheduling optimization in *Case 2*.

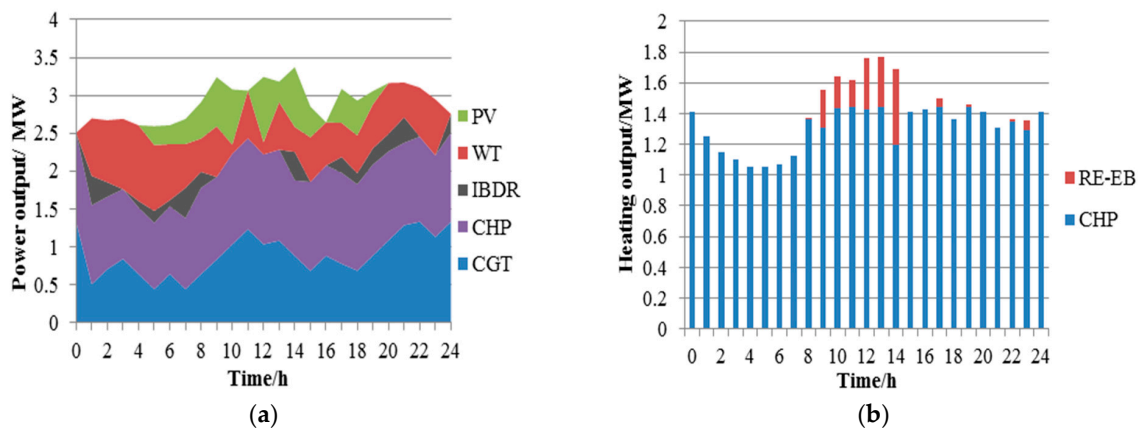


Figure 10. The results of HES operation after application of PBDR (a) and RE-HS (b) in Case 2.

As seen in Figure 10, the grid connection of WT and PV increases obviously after PBDR. WT’s total grid connected power is 13.894×10^3 kWh and PV’s total grid-connected power is 6.503×10^3 kWh. The waste energy values of WT decrease 0.319×10^3 kWh and PV decrease 0.086×10^3 kWh. Both more meet the power needs, which decreases the power for RE-EB, so the heating demand is mainly satisfied by CHP. Accordingly, the power output of CHP also increases as needed. However, the heating output of RE-EB decrease from 2.499×10^3 kWh to 1.958×10^3 kWh, which is mainly concentrated during the peak load periods. Because the power output of WT and PV increases, the revenue and load fluctuation of HES operation increase by 52474.01 ¥ and 0.269×10^3 kW, respectively. In general, PBDR improves the revenue of HES operation, but higher grid connection of WT and PV can also lead to higher load fluctuation, which requires decision makers to make balanced decisions according to their actual situations.

6.2.3. Self-Scheduling of HES in Case 3

Case 3 can analyze the optimization effect of adding RE-HS in HES operation. HS can convert surplus electricity, especially from WT and PV, to storage heating in during the valley period. Then, heating is released during peak load periods to obtain increased economic returns. The weight coefficients of F1 and F2 are 0.76 and 0.24 in Case 3. The economic revenue and load fluctuation of HES operation are 53259.95 ¥ and 0.273×10^3 kW, which are 292.92 ¥ and 0.02×10^3 kW more than those in Case 1, respectively. These results also indicate that RE-HS can increase the operation revenue and risk level. Figure 11 shows the scheduling results of HES operation for Case 3.

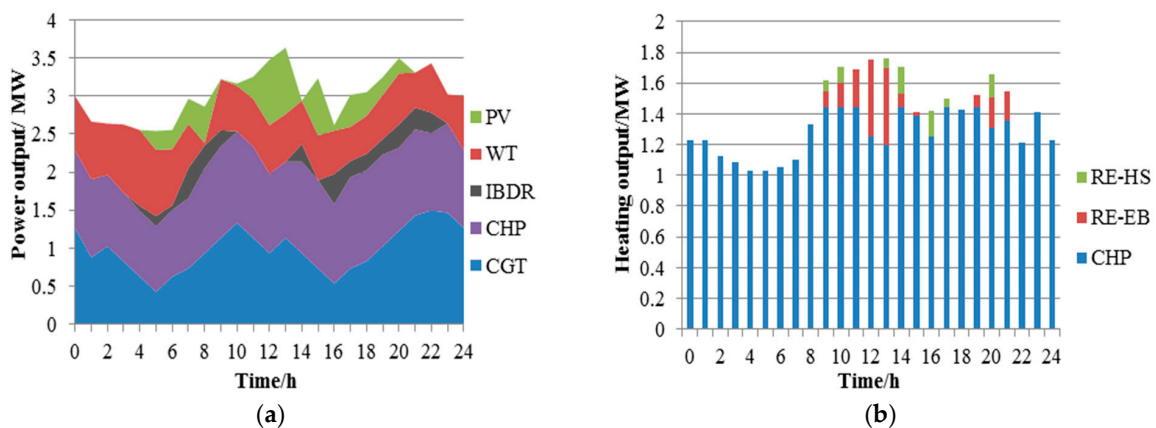


Figure 11. Scheduling result of HES operation after application of PBDR (a) and RE-HS (b) for Case 3.

As seen in Figure 11, during peak load, the output power of the WT and PV increases significantly. The waste energy values of the two are 1.118×10^3 kWh and 2.18×10^3 kWh, respectively. Compared with *Case 1*, WT decreases 1.277×10^3 kWh, and PV decreases by 0.113×10^3 kWh. This is because RE-HS can convert surplus power to heating energy during peak load. Correspondingly, the heating output of CHP reduced by 0.384×10^3 kWh contrast with *Case 1*, but in order to provide reserves, CGT increases its output power from 23.077×10^3 kWh to 23.492×10^3 kWh. Compared with *Case 1*, the output power of WT and PV and reserve demand in *Case 3* have increased. Compared with *Case 1*, due to the significant increase in the output power of WT and PV, the reserve demand also increases, which makes IBDR's efforts more concentrated during peak load periods and float load periods. In general, RE-HS can not only increase the absorption of WT and PV but also increase the operating income of HES. Figure 12 shows the scheduling results of RE operation for *Case 3*.

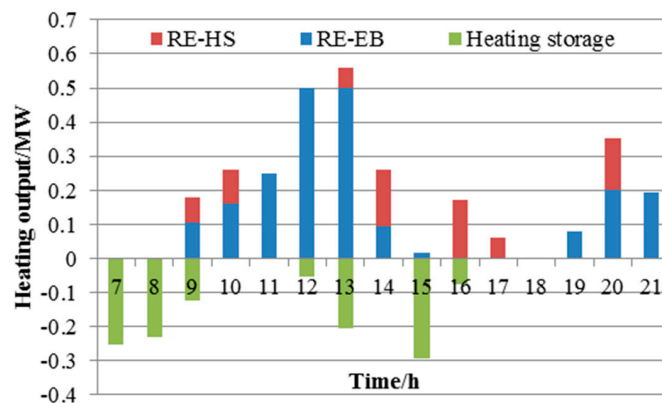


Figure 12. Scheduling results of regenerative electric (RE) operation for *Case 3*.

As seen in Figure 12, RE-HS mainly stores heat during the valley load period (7:00–9:00) and float load period (12:00–16:00). The heating source is mainly the waste energy of WT and PV during floating load. The heat is mainly released during peak load periods, and some of the heat is released during the float load period. Meanwhile, RE-EB releases heat during the float load period (9:00–15:00) and only releases heat during part of the peak load period (18:00–21:00). Obviously, RE-HS can connect the power subsystem and heating subsystem. Heating can be stored when the available output of WT and PV are high and released during peak load periods. Meanwhile, RE-EB can convert power to heat according to the heating load demand. The coordinated operation of RE-HS and RE-EB not only makes full use of WT and PV, but also better meets heating energy demand. Furthermore, the objective function values under different RE scales are analyzed. Figure 13 shows the objective values of HES operation with various RE capacities.

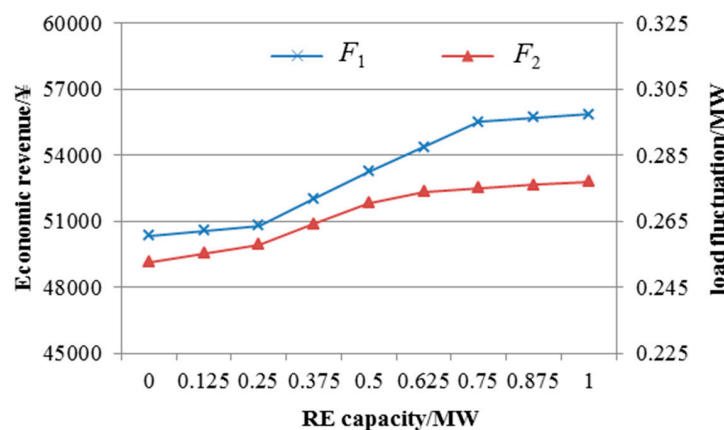


Figure 13. Objective values of HES operation with various RE capacities.

As seen in Figure 13, the objective values of HES operation increase with increasing RE capacity. When the capacity of RE is less than 0.125×10^3 kW, the increase of the objective value is relatively small. This is because when RE capacity is low, the capacity of absorbing WT and PV is limited; thus, the contribution for the objective function value is low. When the capacity of RE is higher than 0.75×10^3 kW, the objective function value increases less. This is because when RE capacity is high enough, the capacity of absorbing WT and PV reaches the upper limit. When the capacity of RE is between 0.25×10^3 kW and 0.625×10^3 kW, with the increase in RE capacity, the objective function value rises quickly, and the power output of WT and PV also increases. This indicates that, for economical and rational HES operation, decision makers must set a reasonable RE capacity according to their actual situations. When the capacity is too low, the desired effect is difficult to achieve. When the capacity is too high, investment waste may occur.

6.2.4. Self-Scheduling of HES in Case 4

Case 4 was mainly used to analyze the optimization scheduling result of HES operation after application of RE-HS and PBDR. PBDR not only balances the load demand curve but also provides more space for HES to absorb WT and PV. RE can convert power into heating according to the heating load demand. Especially during the night, more power output of WT can be converted to storage heating energy. During the peak load periods, heating can be released. In general, both RE and PBDR may increase the grid space of WT and PV. Correspondingly, the economical revenue and load fluctuation of HES operation are 53311.05 ¥ and 0.270×10^3 kW, respectively, which are 2974.02 ¥ and 0.017×10^3 kW more than those in Case 1. Figure 14 shows the scheduling results of HES operation for Case 4.

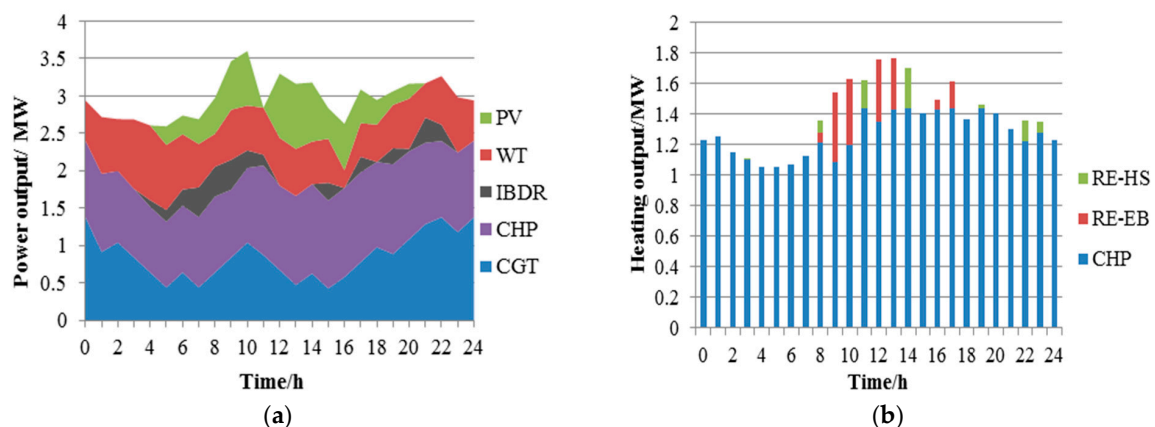


Figure 14. Scheduling results of HES operation after application of PBDR (a) and RE-HS (b) for Case 4.

As seen in Figure 14, when PBDR and RE are applied together, the HES can absorb more power output of WT and PV. Correspondingly, the waste energy of WT and PV decrease 0.798×10^3 kWh and 1.307×10^3 kWh, respectively, which are 1.597×10^3 kWh and 0.986×10^3 kWh lower than those in Case 1. Similarly, since PBDR is implemented, IBDR's efforts are focused on the peak load period, which mainly provides reserve services for WT and PV. However, the power output of CGT decreases by 2.992×10^3 kWh, which indicates that the reserve demand from CGT also decreases. Furthermore, RE-HS converts the surplus power (especially WT and PV) to heating energy, and CHP is mainly used to satisfy the surplus heating demand. Since PBDR has the function of peaking and grain filling, the heating load significantly decreases during some peak load periods. Thus, the output of CHP and RE-HS decreases. Note that RE-EB no longer provides heating during the non-peak load periods. Only RE-HS provides heating at 22:00 and 24:00. Table 3 shows a comparison of Case 3 and Case 4 RE scheduling results.

Table 3. Comparison of *Case 3* and *Case 4* regenerative electric (RE) scheduling results.

Scenario	Heating Output/ $\times 10^3$ kW		Heating Storage/ $\times 10^3$ kWh			Waste Energy/ $\times 10^3$ kWh		RE Revenue/¥
	RE-EB	EB-HS	Peak Load	Float Load	Valley Load	WT	PV	
<i>Case 3</i>	2.105	0.784	0.154	0.355	0.504	1.118	2.180	686.71
<i>Case 4</i>	1.932	0.767	0	0.425	0.584	0.798	1.30	642.37

As seen in Table 3, the heating output of RE operation is reduced from 686.71×10^3 kWh to 642.37×10^3 kWh while the waste energy of WT and PV is also reduced. This indicates that WT and PV are scheduled more to satisfy power load demands, which improves system energy efficiency. Energy loss will occur in the process of converting power into heating and more revenue will be gained because the power price is higher than the heating price. Thus, since the heating outputs of RE-EB and RE-HS both decrease, PBDR indeed changes the energy supply mode. WT and PV output power can not only meet the power load requirements but also bring higher economic benefits. RE mainly uses the waste energy of WT and PV to provide heating, which makes the overall result more reasonable. Correspondingly, RE-HS mainly stores heat during load valley period and floating period, while RE-HS has a heating storage capacity of 0.154×10^3 kWh in *Case 3* during peak load periods.

6.3. Results Analysis

The scheduling results of the above cases demonstrate that both PBDR and RE-HS have direct impacts on HES operation. The former can change the load demand curve of power and heating to influence the scheduling plan of various HES components. The latter can be used to maintain energy balance by releasing heat stored during the load of the valley during peak periods. Furthermore, to analyze the scheduling results of HES operation in various scenarios, we comparatively analyze three aspects of the scheduling results, the net load curve, and IBDR operation result. Table 4 shows HES scheduling optimization results for different cases.

Table 4. HES scheduling optimization results for different cases.

Scenario	Weight		Power Output/ $\times 10^3$ kWh					Heating Output/ $\times 10^3$ kWh			Objective Value	
	F1	F2	CGT	WT	PV	CHP	IBDR	CHP	RE-EB	RE-HS	F1/¥	F2/ $\times 10^3$ kW
<i>Case 1</i>	0.78	0.22	23.077	13.575	6.417	25.897	5.694	31.074	2.499	-	50337.03	0.253
<i>Case 2</i>	0.72	0.28	21.044	13.894	6.503	26.046	5.616	31.256	1.958	-	52474.01	0.269
<i>Case 3</i>	0.76	0.24	23.492	14.853	6.530	25.555	5.285	30.663	2.105	0.784	53259.95	0.273
<i>Case 4</i>	0.75	0.25	20.085	15.172	7.403	25.394	5.122	30.476	1.932	0.767	53311.05	0.268

First, the weight of the objective function, the weights of F1 in the other three cases are lower than that in *Case 1*. This is because both PBDR and RE-HS add the grid connection for WT and PV, which results in the load fluctuation becoming stronger. It is necessary to increase the weight of F2 to achieve economical and stable HES operation. Furthermore, the value of F1 in *Case 4* reaches the maximum, while the value of F2 in *Case 1* reaches the minimum. The values in *Cases 2* and *4* are smaller than that in *Case 3*, which indicates that RE-HS and PBDR can maximize the operation revenue. On the other hand, the grid connection space of WT and PV is increased by adding RE-HS and PBDR, resulting in significantly increased load fluctuations, but PBDR can not only be a smoother load demand curve but also optimize the operation results of RE-HS. Therefore, there is less load fluctuation in *Case 4* than in *Cases 2* and *3*. In general, RE-HS and PBDR can improve the economical revenue of HES operation, but they also increase the load fluctuation. However, when they are both applied, the load fluctuation decreases. This indicates that RE-HS and PBDR have combined optimization effects. Figure 15 shows the net power load demand in various cases.

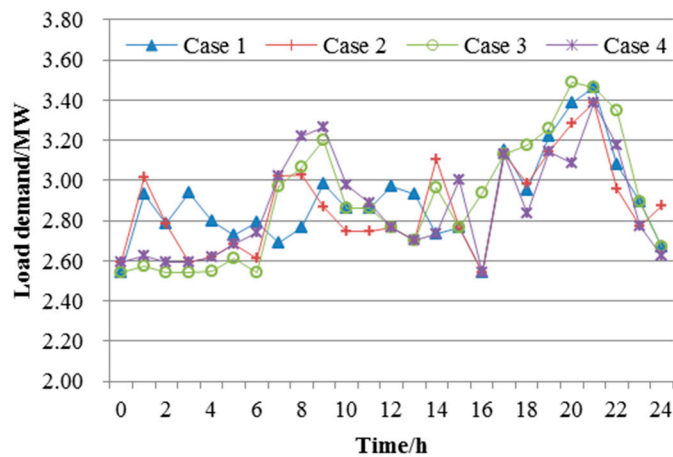


Figure 15. Net power load demand curve in various cases.

As seen in Figure 15, in comparison with *Case 1*, the peak load is 3.387×10^3 kW and the valley load is 2.541×10^3 kW, and the peak-to-valley ratio is 1.333. The power load curve in *Case 3* is the steepest. Peak and valley loads are 3.486×10^3 kW and 2.539×10^3 kW, respectively, and the peak-to-valley ratio is 1.373. However, the peak–valley ratios in *Cases 2* and *4* are 1.363 and 1.343, respectively, which shows that RE-HE can play the role of cutting peaks and filling valleys. Moreover, PBDR plays a role in reducing peak load and peak-to-valley ratio. When RE-HS and PBDR are both applied, the peak-to-valley ratio is 1.333, which indicates that RE-HS and PBDR have combined optimization effect. Furthermore, the operation situations of IBDR in various cases are considered, especially the scheduling results of IBDR contributing to energy scheduling and reserve scheduling. Figure 16 shows the power distributions of IBDR scheduling in various cases.

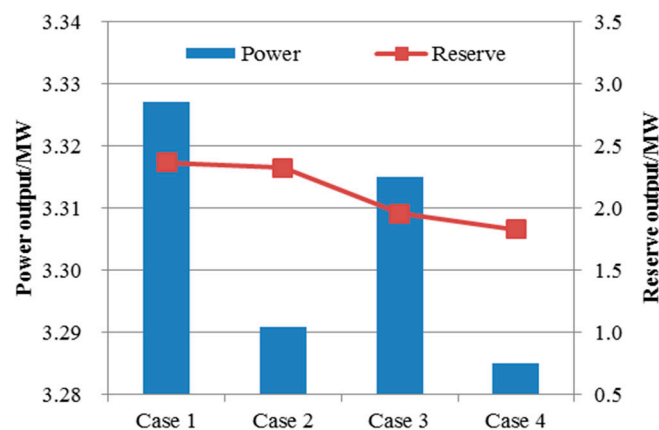


Figure 16. Power distribution of incentive-based demand response (IBDR) scheduling in various cases.

As seen in Figure 16, the scheduling output values of IBDR in the energy and electricity reserve market in *Cases 2* and *3* are lower than those in *Cases 1* and *4*. The power output of IBDR scheduling in the energy market are 3.327×10^3 kWh, 3.291×10^3 kWh, 3.315×10^3 kWh, and 3.285×10^3 kWh, respectively. This shows that PBDR can reduce the reserve demand of IBDR by balancing the load demand curve. Further, comparing *Case 2* with *Case 3* shows that when RE-HS and PBDR are both applied, the scheduling output of IBDR in the energy and electricity reserve market reach the lowest levels. This is because the application of both RE-HS and PBDR makes the load curve flatter. RE-HS mainly takes advantage of the waste energy of WT and PV to satisfy the heating demand, which decreases the system upper reserves. Therefore, the reserve output of IBDR scheduling reaches the lowest level.

The simulation results show that the optimized control method proposed in this paper can effectively improve the utilization efficiency of the energy system to abandon the wind, extend the service life of the equipment, and improve the system economy. It provides more flexibility for P2G equipment to participate in the abandonment of wind consumption, economic operation methods and theoretical basis.

In the day-to-day scheduling of integrated energy systems with P2G, this paper considers the impact of P2G operating costs on system wind power acceptance and operational economy, and proposes a multi-objective optimization model to coordinate the contradiction between the two. The results of the example show that the higher P2G operating cost will affect the wind power acceptance capability and operational economy of the system to a certain extent, which will cause certain contradictions between the two; however, the multi-objective model proposed in this paper can take into account the system operation. Economic and wind power acceptance capabilities and a variety of options for scheduling decisions. In the follow-up work, the model will be further refined, such as considering wind power prediction error, gas network dynamic characteristics, etc. In addition, it will also expand the flexibility of the research system in terms of “source” and “charge”, such as multi-energy time-sharing pricing, consideration Use alternative comprehensive demand response.

7. Conclusions

To satisfy the load demand for power and heating, WT, PV, CGT, IBDR, RE, CHP are integrated into build a HES. The collaborative optimization problem of HES was discussed. Firstly, based on the objective function of HES maximum working income and minimum load fluctuation, a multi-objective optimization model of HES scheduling is proposed. Secondly, the linearization method of the objective function and the constraint and the weight calculation method of the objective function are proposed to solve the objective function. Finally, based on whether RE-HS and PBDR are used, four simulation schemes are proposed. Taking an island in eastern China as an example, the microgrid is used as a simulation system to verify the effects of the proposed model and algorithm. The results are as follows:

- (1) HES can meet the load demand by making full use of DER. RE can not only convert the waste energy of WT and PV in the load valley period into heat energy, but also cooperate with CHP to meet the heating needs. In FTL mode, the main heat source is CHP, the main power source is CHP, WT and PV. WT and PV reserve IBDR and CGT can be provided. The difference is that IBDR is mainly concentrated in the period of load peak, and CGT is in the period of load valley.
- (2) The proposed HES operation multi-objective scheduling model can maximize operational benefits and minimize load fluctuations. Under the optimal operation revenue mode, the values of F1 and F2 are 50837.03 ¥ and 0.275×10^3 kW, respectively. Under the optimal load fluctuation mode, the values of F1 and F2 are 49852.45 ¥ and 0.246×10^3 kW, respectively. Under the integrated optimization mode, the values of F1 and F2 are 50337.03 ¥ and 0.253×10^3 kW. In comparison with the single-objective optimization mode, the objective function value of the integrated optimization mode can better consider the two optimization models and achieve optimal equilibrium HES operation.
- (3) RE-HS and PBDR have a synergistic optimization effect and can achieve optimal results of HES operation. Compared with the cases of HES scheduling with RE-HS or PBDR alone, when both of them are applied, the values of F1 and F2 in *Case 1* increase from 50337.03 ¥ and 0.253×10^3 kW to 53311.05 ¥ and 0.268×10^3 kW in *Case 4*. The power output values of WT and PV increase from 13.575×10^3 kWh and 6.417×10^3 kWh in *Case 1* to 15.172×10^3 kWh and 7.403×10^3 kWh. The peak-to-valley ratio reaches the minimum, 1.333. Correspondingly, the power output of IBDR reaches the minimum in *Case 4*.
- (4) This paper focused on the aggregation utilization problem of WT, PV, CGT, and other distributed power sources with CHP, a multi-objective scheduling model and its corresponding algorithm are proposed. The simulation results also prove that the proposed model and algorithm are effective. However, the strong uncertainty of WT and PV directly influence the optimal decisions

for HES operation. This problem should be investigated further and will be the focus of our future research.

In the daily dispatching of P2G integrated energy system, considering the impact of P2G operating cost on system wind power acceptance and operational economy, this paper proposes a multi-objective optimization model to coordinate the contradiction between the two. It can balance the economics of system operation with wind power acceptance and provide a variety of options for scheduling decisions. In the follow-up work, the model will be further refined, such as considering wind power prediction error, gas network dynamic characteristics, etc. In addition, it will also expand the flexibility of the research system in terms of “energy” and “load”, such as multi-energy time-sharing pricing, consideration Use alternative comprehensive demand response.

Author Contributions: Data curation, Z.T.; Methodology, T.W. and Q.T.; Writing—original draft, Y.W., L.J. and J.W.; Writing—review & editing, Y.L.

Funding: This work was partially supported by Supported by the Science Foundation of China University of Petroleum, Beijing (No. ZX20170256), the National Science Foundation of China (Grant Nos. 71273090), and the Beijing Social Science Fund(18GLC058).

Conflicts of Interest: The authors declare no conflict of interest.

Nomenclature

DERs	distributed energy
RE	regenerative electric
CHP	combined heat and power
VPP	virtual power plant
HES	hybrid energy system
IBDR	incentive demand response
FTL	follow-up electrical load
TOU	time-of use
MGs	micro-grids
WTs	wind turbine
PV	photovoltaic
v	the real-time wind speed
φ	the form factor
ϑ	the scale factor
g_W^*	the maximum output of the WT
g_R	the WT rated output
v	the real-time wind velocity
t	time
θ	the solar radiation intensity
α, β	the shape parameters of the beta distribution
u	the expected value of the PV radiation intensity
σ	the standard deviations of the PV radiation intensity
g^*	output power
η_{PV}	efficiency
S	total area
θ	radiation intensity
$D_i^{j,\min}$	the minimum demand response
$D_i^{j,\max}$	the largest demand response
ΔL_i	actual load reduction
j	the step
D_i	available load reduction
ΔL_{IB}	the output power provided by IBDR

$g_{CHP,t}^h$	the supply of heating power of CHP at time t
$g_{CHP,t}^e$	the supply of electricity power of CHP at time t
$g_{CHP}^{h,max}$	the maximum heating power supply
$g_{CHP}^{e,min}$	the minimum values of CHP power supply under pure condensation conditions
$g_{CHP}^{e,max}$	the minimum values of CHP power supply under pure condensation conditions
$g_{CHP}^{e,min}$	the minimum heating power of CHP corresponding to the minimum electricity power
c_{max}, c_{min}	the linear supply slopes of heating power and electric power of CHP
$g_{CHP}^{e,min}$	the minimum electricity power of CHP
$g_{CHP}^{h,m}$	the heating power of CHP when the electric power reaches the minimum value
g_{EB}^{RE}	the electric power for the heating supply of RE-EB
Q_{EB}^{RE}	the heating power supply of RE-EB
η_{EB}^{RE}	the efficiency of thermal–electrical conversion
S_{HS}^{RE}	the storage capacity for RE-HS
φ_{HS}	the heat dissipation loss rate of HS
Q_{HS}^{RE}	the heating power used for RE-HS
Q_{HS}^{out}	the exothermic power for RE-HS
$\eta_{HS}^{in}, \eta_{HS}^{out}$	the endothermic and exothermic efficiency
F_1	the objective function of HES operation net revenue
R	the operating income
ρ	the price of buying electricity from the grid
g	the amount of electricity purchased
C	the cost of power generation
pg	start
ss	close
a, b, c	the cost coefficients
u	the operation status
N_{CGT}^{hot} and N_{CGT}^{cold}	the CGT cold and hot startup costs
T	the operating time
ρ	the output price
f	the cost function
C	the cost of power generation
sd	startup–shutdown
t, s	the indexes for time
ρ	the grid-prices
e	power
h	heating
g	the output
θ_h^e	the thermal–electricity conversion coefficient of CHP
ρ_{RE}^e	the prices for power
ρ_{RE}^k	the prices for heating
Q_{RE}	the heating output of RE
g_{RE}	the power input of RE
F_2	the objective of HES load fluctuation
$\bar{g}_{VPP,t}$	the average load fluctuation for the HES throughout the entire scheduling period
$(\Delta L_{IB,t}^- - \Delta L_{IB,t}^+)$	the net output of IBDR
$\varphi_{WPP}, \varphi_{PV},$ and φ_{CHP}	the power loss rates
$g_{UG,t}$	the electricity purchased from the grid
g_{EB}^{RE}	the input electricity of RE-EB
g_{HS}^{RE}	the input electricity of RE-HS
μ_{IB}	the status variables of IBDR
μ_{PB}	the status variables of PBDR
Δ	the amount of change after adding PBDR
L	the demand
P	the price

L_t^0	the load demand before PBDR
L_t	the load demand after PBDR
P_t^0	the electricity price before PBDR
P_t	the electricity price after PBDR
e_{st}	the elasticity of price and demand
Q	the heating demand of terminal customers
Q^{out}	the heating output
u_{PB}^h	the status variable of implementing PBDR for the heating load
ΔQ	the amount of load change before and after adding PBDR
$g_{CGT}^{\min}, \Delta g_{CGT}^+$	the upper limits of CGT
$g_{CGT}^{\max}, \Delta g_{CGT}^-$	the lower limits of CGT
$\Delta L_{IB}^{up}, \Delta L_{IB}^{dn}$	the maximum and minimum reserve outputs of IBDR in the reserve market
$\Delta L_{IB}^{\max}, \Delta L_{IB}^{\min}$	the maximum and minimum output of IBDR
g_{NE}	the output of NE
g_{NE}^*	the revised output of NE
g_{CHP}	the output of CHP under the working condition of the pure condensing condition
Q_{RE}^{\max}	the maximum output of RE
$S_{HS,0}^{RE}, S_{HS,T}^{RE}$	the storage heating by the HS at the beginning and end of the schedule
$S_{HS}^{RE,\min}, S_{HS}^{RE,\max}$	the minimum and maximum capacities of HS under stable operation condition
$Q_{HS,nom}$	the rated capacity of HS
$g_{MES}^{\max}, g_{MES}^{\min}$	the maximum and minimum values of the HES output
$r_1, r_2, \text{ and } r_3$	the upper reserve factors of power load, WT, and PV
r_4, r_5	the lower reserve factors of WT and PV
r_6, r_7	the upper and lower reserve coefficients of the heating load
U^0	the time period of CGT operation at the start of the scheduling period
α_1, α_2	set

References

1. Mashhour, M.; Golkar, M.A.; Moghaddas-Tafreshi, S.M. Extending Market Activities for a Distribution Company in Hourly-ahead Energy and Reserve Markets—Part I: Problem Formulation. *Energy Convers. Manag.* **2011**, *52*, 477–486. [CrossRef]
2. David, S.; Arturs, P.; Ioulia, P. Benefits and Cost Implications from Integrating Small Flexible Nuclear Reactors with Off-shore Wind Farms in a Virtual Power Plant. *Energy Policy* **2012**, *46*, 558–573.
3. Wei, H.K.; Liu, J.; Yang, B. Cost-benefit Comparison Between Domestic Solar Water Heater (DSHW) and Building Integrated Photovoltaic (BIPV) Systems for Households in Urban China. *Appl. Energy* **2014**, *126*, 47–55. [CrossRef]
4. Wang, Q.; Zhang, C.Y.; Ding, Y. Review of Real-time Electricity Markets for Integrating Distributed Energy Resources and Demand Response. *Appl. Energy* **2015**, *138*, 695–706. [CrossRef]
5. European Virtual Fuel Cell Power Plant Management Summary Report [EB/OL]. 2012-08-13. Available online: <http://ec.europa.eu/energy/efficiency/industry/doc/euvpp.pdf/> (accessed on 13 August 2012).
6. Rossi, F.; Velazquez, D. A Methodology for Energy Savings Verification in Industry with Application for a CHP (Combined Heat and Power) plant. *Energy* **2015**, *89*, 528–544. [CrossRef]
7. Ju, L.; Tan, Z.; Yuan, J.; Tan, Q.; Li, H.; Dong, F. A Bi-level Stochastic Scheduling Optimization Model for a Virtual Power Plant Connected to a Wind-Photovoltaic-Energy Storage System Considering the Uncertainty and Demand Response. *Appl. Energy* **2016**, *171*, 184–199. [CrossRef]
8. Tan, Z.F.; Wang, G.; Ju, L.W.; Tan, Q.K.; Yang, W.H. Application of CVaR Risk Aversion Approach in the Dynamical Scheduling Optimization Model for Virtual Power Plant Connected with Wind-Photovoltaic-Energy Storage System with Uncertainties and Demand Response. *Energy* **2017**, *124*, 198–213. [CrossRef]
9. Tan, Z.F.; Zhang, H.J.; Shi, Q.S.; Song, Y.H.; Ju, L.W. Multi-objective Operation Optimization and Evaluation of Large-scale NG Distributed Energy System Driven by Gas-steam Combined Cycle in China. *Energy Build.* **2014**, *76*, 572–587. [CrossRef]

10. Yu, S.; Wei, Z.; Sun, G.Q.; Sun, Y.; Wang, D. A Bidding Model for a Virtual Power Plant Considering Uncertainties. *Autom. Electric Power Syst.* **2014**, *38*, 44–49.
11. Project Interim Report[R/OL]. 20 February 2013. Available online: <http://www.web2energy.com/> (accessed on 20 February 2013).
12. Zapata, J.; Vandewalle, J.; D'haeseleer, W. A Comparative Study of Imbalance Reduction Strategies for Virtual Power Plant Operation. *Appl. Thermal Eng.* **2014**, *71*, 847–857. [[CrossRef](#)]
13. Saeed, R.D.; Mohammad, K.S. Risk-based Profit Allocation to DERs Integrated with a Virtual Power Plant Using Cooperative Game Theory. *Electrical Power Syst. Res.* **2015**, *121*, 368–378.
14. Moghaddam, I.G.; Nick, M.; Fallahi, F.; Sanei, M.; Mortazavi, S. Risk-averse Profitbased Optimal Operation Strategy of a Combined Wind Farm-Cascade Hydro System in an Electricity Market. *Renew. Energy* **2013**, *55*, 252–259. [[CrossRef](#)]
15. Pandzic, H.; Kuzle, I.; Capuder, T. Virtual Power Plant Mid-term Dispatch Optimization. *Appl. Energy* **2013**, *101*, 134–141. [[CrossRef](#)]
16. Wang, Y.; Ai, X.; Tan, Z.; Yan, L.; Liu, S. Interactive Dispatch Modes and Bidding Strategy of Multiple Virtual Power Plants Based on Demand Response and Game Theory. *IEEE Trans. Smart Grid* **2015**, *9*, 1–10. [[CrossRef](#)]
17. Carrion, M.; Arroyo, J.M. A Computationally Efficient Mixed-integer Linear Formulation for the Thermal Unit Commitment Problem. *IEEE Trans. Power Syst.* **2006**, *21*, 1371–1378. [[CrossRef](#)]
18. Erdinc, O. Economic Impacts of Small-scale Own Generating and Storage Units and Electric Vehicles Under Different Demand Response Strategies for Smart Households. *Appl. Energy* **2014**, *126*, 142–150. [[CrossRef](#)]
19. Aboelsood, Z.; Hossam, A.G.; Ahmed, E. Optimal Planning of Combined Heat and Power Systems within Microgrids. *Energy* **2015**, *93*, 235–244.
20. Zhang, N.; Wang, Z.F.; Noam, L.; Wei, H. Advancement of Distributed Energy Methods by a Novel High Efficiency Solar-Assisted Combined Cooling, Heating and Power System. *Appl. Energy* **2019**, *218*, 179–186. [[CrossRef](#)]
21. Aluisio, B.; Dicorato, M.; Forte, G.; Trovato, M. An Optimization Procedure for Microgrid Day-Ahead Operation in the Presence of CHP facilities. *Sustain. Energy Grids Netw.* **2017**, *11*, 34–45. [[CrossRef](#)]
22. Taher, N.; Rasoul, A.A.; Alireza, R.; Babak, A. A New Multi-objective Reserve Constrained Combined Heat and Power Dynamic Economic Emission Dispatch. *Energy* **2012**, *42*, 530–545.
23. Mohammad, R.R.; Mohsen, M.; Saied, E. Economic Analysis of Hybrid System Consists of Fuel Cell and Wind Based CHP System for Supplying Grid-Parallel Residential Load. *Energy Build.* **2014**, *68*, 476–487.
24. Wille, H.B.; Erge, T.; Wittwer, C. Decentralised Optimisation of Cogeneration in Virtual Power Plants. *Solar Energy* **2010**, *84*, 604–611. [[CrossRef](#)]
25. Giuntoli, M.; Poli, D. Optimized Thermal and Electrical Scheduling of a Large Scale Virtual Power Plant in the Presence of Energy Storages. *IEEE Trans. Smart Grid* **2013**, *4*, 942–955. [[CrossRef](#)]
26. Manijeh, A.; Kazem, Z.; Heresh, S. A Multi-follower Bilevel Stochastic Programming Approach for Energy Management of Combined Heat and Power Micro-Grids. *Energy* **2018**, *149*, 135–146.
27. Aalami, H.A.; Pashaei-Didani, H.; Nojavan, S. Deriving nonlinear models for incentive-based demand response programs. *Int. J. Electrical Power Energy Syst.* **2019**, *106*, 223–231. [[CrossRef](#)]
28. Eissa, M.M. First time real time incentive demand response program in smart grid with “i-Energy” management system with different resources. *Appl. Energy* **2018**, *212*, 607–621. [[CrossRef](#)]
29. Eissa, M.M. Developing incentive demand response with commercial energy management system (CEMS) based on diffusion model, smart meters and new communication protocol. *Appl. Energy* **2019**, *236*, 273–292. [[CrossRef](#)]
30. Guo, Y.H.; Hu, B.; Wan, L.Y.; Xie, K.G.; Yang, H.J.; Shen, Y.M. Optimal Economic Short-term Scheduling of CHP Microgrid Incorporating Heat Pump. *Autom. Electric Power Syst.* **2015**, *39*, 16–22.
31. Ju, L.W.; Li, H.H.; Zhao, J.W. The Multi-objective Stochastic Scheduling Optimization Model for Connecting a Virtual Power Plant with Wind-Photovoltaic-Electric Vehicles Considering Uncertainties and Demand Response. *Energy Convers. Manag.* **2016**, *128*, 160–177. [[CrossRef](#)]

